Single-Gate Bandgap Opening of Bilayer Graphene by Dual Molecular Doping

Jaesung Park, Sae Byeok Jo, Young-Jun Yu, Youngsoo Kim, Jae Won Yang, Wi Hyoung Lee, Hyun Ho Kim, Byung Hee Hong, Philip Kim, Kilwon Cho, and Kwang S. Kim**

Graphene has attracted much attention because of its exceptional physical properties such as an anomalous quantum hall effect[1,2] and Klein tunneling[3] originating from a chiral fermion. In addition, graphene-based electronic devices have been designed to exhibit high carrier mobility,[4] ultrahigh speed,[5,6] large scale flexibility,[7,8]and fast DNA sequencing.[9,10] However, due to the absence of a bandgap, pristine graphene devices cannot be switched off, which poses a great challenge for digital electronic device applications. To overcome this disadvantage, several approaches including fabrication of graphene nanoribbons[11,12] and implanting periodic heteroatoms on a graphene lattice have been applied to engineer energy gap in graphene.[13,14]

On the other hand, bilayer graphene serves a unique alternative for bandgap engineering by applying a perpendicular electric field for breaking the inversion symmetry of graphene.[15] For instance, a gate-controlled tunable bandgap of a bilayer graphene has been successfully demonstrated by fabricating field-effect transistors (FETs) with dual-gate structure.[16–20] Chemical treatment of graphene might be a facile approach for the engineering of band structure with chemical functionality.[21] An alternative purely chemical approach to generating a built-in perpendicular electric field is also possible. For example, deposition of a chemical dopant on top of bilayer graphene has been shown to induce a perpendicular electric field in a similar way as applying a gate voltage.[22,23] In this approach, however, controlled doping was only applied to the top layer of graphene and thus it was difficult to tune the charge carrier density and bandgap independently. If the bottom layer as well as top layer can be doped in a controllable manner, there should be the possibility to fabricate single-gate graphene FETs with a high on/off current ratio.

Here, we used self-assembled monolayers (SAMs) constructed on silicon substrate as controllable doping of graphene on the bottom side (**Figure 1**a). As an ultrathin layer can be uniformly deposited on the oxide substrate, SAMs have been utilized to treat and functionalize the oxide substrate in graphene electronics.[24–26] In particular, amine (NH_2) functionalized SAMs n-dope graphene due to the electron donating characteristics of the SAM end groups (Figure 1b, bottom). We used aminopropyltriethoxysilane to fabricate NH_2-functionalized SAMs on a SiO_2/Si substrate. The detailed fabrication procedure for SAMs was reported previously.[26] Bilayer graphene was prepared onto NH_2-functionalized SAMs by mechanical exfoliation from Kish graphite. The optical contrast of the exfoliated pieces was used for selecting the bilayer. Furthermore, the Raman spectrum shown in Figure 1c (inset), which exhibits a broad 2D band (full width at half-maximum of ≈55 cm^{-1}) consisting of four distinct peaks, confirms that the obtained species is indeed bilayer.[27] Au (50 nm)/Ti (5 nm) source and drain contacts were fabricated onto bilayer graphene using electron beam (e-beam) lithography. Figure 1c shows bilayer graphene FETs constructed on a NH_2-SAM modified SiO_2 (thickness of 300 nm)/Si substrate.

2,3,5,6-tetrafluoro-7,7,8,8-tetracyanoquinodimethane (F4-TCNQ; Figure 1b, top) was thermally deposited onto bilayer graphene FETs to induce the doping-driven perpendicular electric field from the top. Because F4-TCNQ consists of cyano and fluoro groups with electron withdrawing characteristics, it exhibits a low lying lowest unoccupied molecular orbital (LUMO) level of –5.2 eV.[28] This, in turn, leads to p-doping of graphene when F4-TCNQ is in contact with graphene, which exhibits work function of ≈4.6 eV.[29] As a perpendicular electric field can be applied to graphene by molecular doping using F4-TCNQ, the bandgap opening of bilayer graphene was demonstrated by depositing F4-TCNQ on top of bilayer graphene[23,30] and the same method was used in our experiment. Furthermore, it is expected that the combination of p-doping by depositing F4-TCNQ from the top and n-doping by NH_2-functionalized SAMs at the bottom can induce larger bandgap than by treating only a single doping agent.

Dr. J. Park,[+] Dr. Y.-J. Yu, Dr. W. H. Lee, Prof. K. S. Kim
Center for Superfunctional Materials
Department of Chemistry
Pohang University of Science and Technology
Pohang 790-784, Korea
E-mail: kim@postech.ac.kr
S. B. Jo,[+] Dr. W. H. Lee, H. H. Kim, Prof. K. Cho
Department of Chemical Engineering
Pohang University of Science and Technology
Pohang 790-784, Korea
E-mail: kwcho@postech.ac.kr
Dr. Y.-J. Yu, Prof. P. Kim
Department of Physics
Columbia University
New York, NY 10027, USA
Y. Kim, Prof. B. H. Hong
Department of Chemistry
Sungkyunkwan University
Suwon 440-746, Korea
Prof. B. H. Hong
Department of Chemistry
Seoul National University
151-742, Korea
J. W. Yang
Department of Physics
Pohang University of Science and Technology
Pohang 790-784, Korea
[+] These authors contributed equally to this work.

DOI: 10.1002/adma.201103411

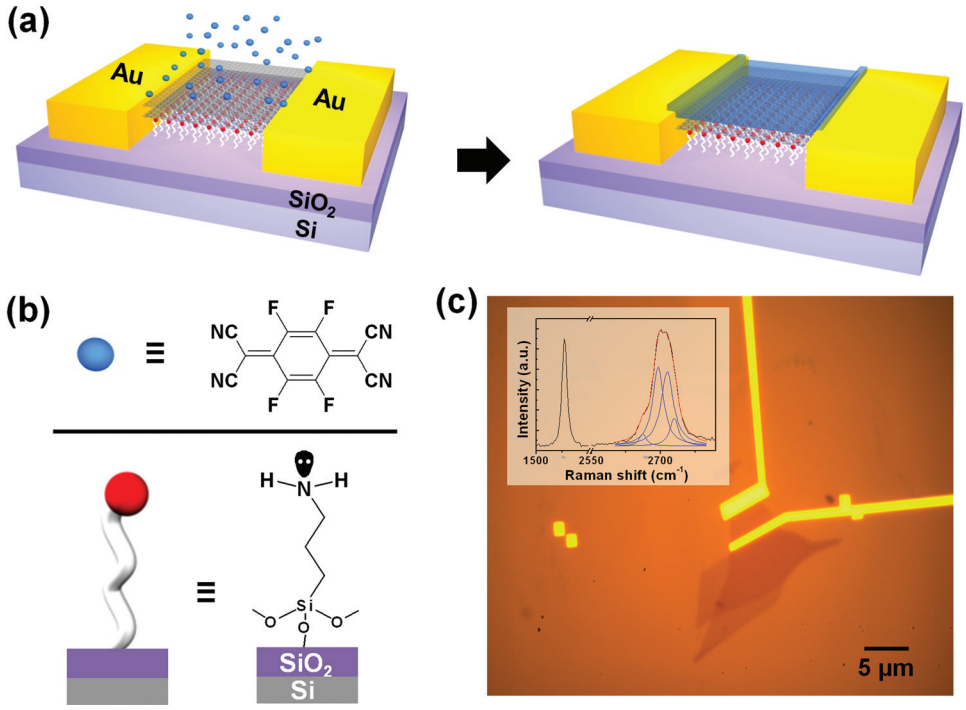

Figure 1. a) Schematic dual doping process for bilayer graphene consisting of both n-doping by aminopropyltriethoxysilane modified SiO_2/Si substrate (bottom) and p-doping by evaporating 2,3,5,6-tetrafluoro-7,7,8,8-tetracyanoquinodimethane (F4-TCNQ) (top). b) Chemical structures of NH_2-functionalized SAMs on a SiO_2/Si substrate (bottom) and F4-TCNQ (top). c) Optical microscopy image of a bilayer graphene FET. The inset shows the Raman spectrum of bilayer graphene on a NH_2-SAM modified SiO_2/Si substrate.

Figure 2a,b show the effects of top/bottom doping on the electrical properties of bilayer and monolayer graphene FETs, respectively. By the incorporation of NH_2-SAMs onto a SiO_2/Si substrate, the Dirac voltages of both the bilayer and monolayer graphene shift to the negative values. This result confirms that graphene is effectively n-doped by NH_2-SAMs. On the other hand, resistances show a different trend. Although the off-resistance of bilayer graphene increases by around two times (from 2.4 to 4.6 kΩ), this value for monolayer graphene does not increase considerably. It is reported that doping by amine groups does not significantly increase the scattering from the charged impurities in monolayer graphene,[31–33] which explains our data observed in monolayer graphene FETs. On the other hand, the increase in resistance in bilayer graphene can be understood in terms of n-doping and bandgap opening of graphene, as schematically drawn in Figure 2c. The subsequent deposition of F4-TCNQ (thickness of 10 Å) onto bilayer graphene leads to huge increase in the off-resistance (≈12.2 kΩ), which implies that p-doping from the top effectively breaks the inversion symmetry of bilayer graphene, thus leading to bandgap opening (see Figure 2c). It is observed that off-resistance of monolayer graphene also increases a little (from 3.9 to 5 kΩ). This might be attributed to the formation of electron–hole puddles after F4-TCNQ deposition by a charged impurity.[34,35] We speculate that inhomogenous morphology of the F4-TCNQ thin film may induce fluctuation in the degree of doping, thus resulting in the formation of disorder-induced electron–hole puddles (Supporting Information Figure S1). Although a charged impurity can also contribute to the increase in off-resistance of the bilayer graphene, the magnitude of the increase in off-resistance is much higher than that of monolayer graphene, confirming the bandgap opening of the bilayer graphene.

To examine the effect of F4-TCNQ thickness on the electrical properties of bilayer graphene FETs on NH_2-SAM modified SiO_2/Si substrates, various thicknesses of F4-TCNQ layers from 0 to 25 Å (nominal thickness) were deposited and the electrical properties were measured as shown in **Figure 3**a. As the thickness of F4-TCNQ layer increases, the Dirac voltage gradually shifts to positive value with an increment rate of 0.85 V $Å^{-1}$, confirming controllable p-doping of graphene. Furthermore, the on/off current ratio linearly increases with an increase of the F4-TCNQ thickness (Figure 3b). The gate-controllable output characteristic becomes obvious as the thickness of the F4-TCNQ layers increases (Supporting Information Figure S3a–c). These characteristics confirm the controllable opening of the bandgap in bilayer graphene through control of the thickness in F4-TCNQ layers (Supporting Information Figure S4). On the other hand, the field-effect mobility calculated in the linear regime for transfer characteristics is inversely proportional to the F4-TCNQ thickness (Supporting information Figure S3d), which is likely due to an increase in the charged impurities by the F4-TCNQ doping.

To estimate the optical bandgap of bilayer graphene with the F4-TCNQ thickness, infrared (IR) absorption spectra of bilayer graphene on NH_2-SAMs modified SiO_2/Si substrate were measured and are shown in Figure 3c. The absorption spectrum of pristine graphene on a bare SiO_2/Si substrate was subtracted as

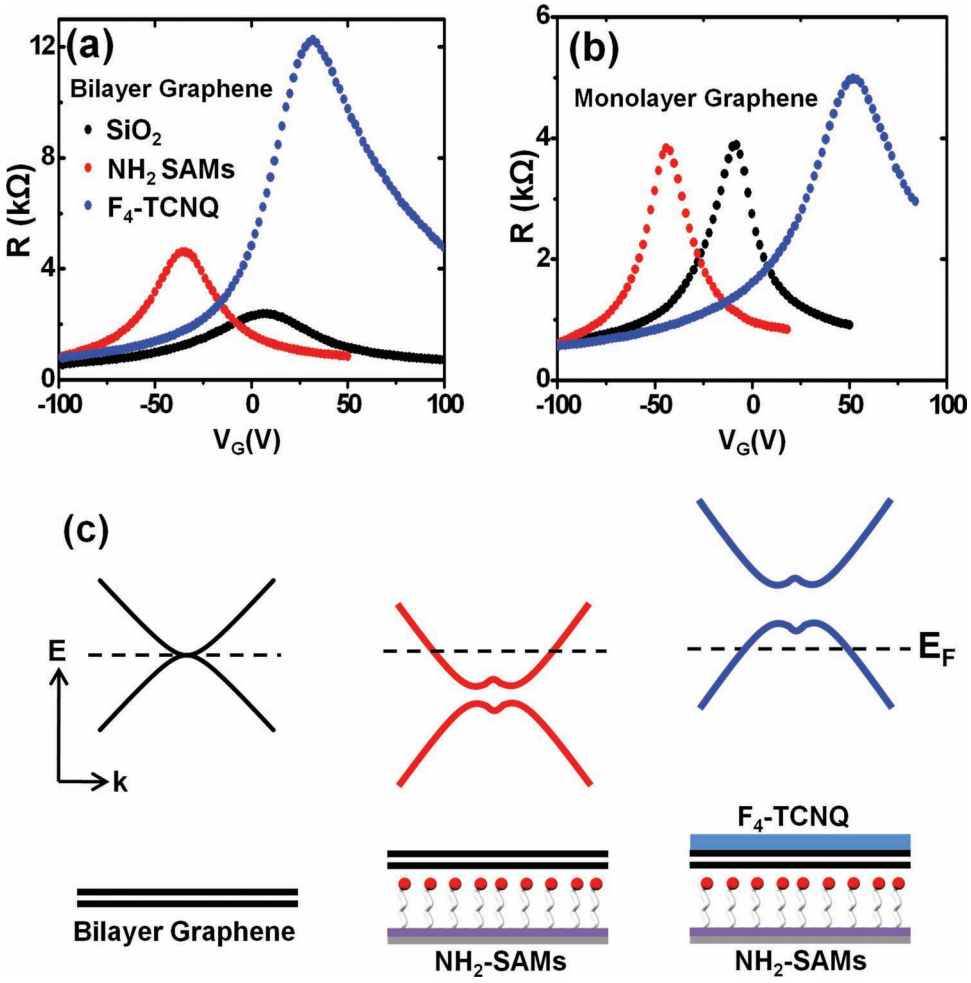

Figure 2. Current–voltage transfer characteristics of a) bilayer graphene FETs and b) monolayer graphene FETs with molecular doping agents. SiO_2: untreated SiO_2/Si (no doping), NH_2: NH_2-SAM modified SiO_2/Si (n-doping), F4-TCNQ: 2,3,5,6-tetrafluoro-7,7,8,8-tetracyanoquino-dimethane (thickness of 10 Å, p-doping). c) The electronic band structures of bilayer graphene on an untreated, NH_2-SAM modified SiO_2/Si substrate and F4-TCNQ deposited bilayer graphene on a NH_2-SAM modified SiO_2/Si substrate (shown from left to right).

a background reference. The spectra show three clear features around 130 meV, 200 meV, and 400 meV. The sharp absorption peak at 130 meV, which shows a gradual increase in the peak intensity with an increase in F4-TCNQ thickness, may correspond to the vibration of C–F from F4-TCNQ. The absorption peak around 160 to 210 meV, which exhibits a positive relation with F4-TCNQ thickness, is explained by the optical transition from the valence band to the conduction band in bilayer graphene.[18] This tunable bandgap transition is linearly proportional to the F4-TCNQ thickness, which experimentally proves that F4-TCNQ doping opens a bandgap in a controllable manner (Figure 3d). A dip centered around 400 meV is likely due to the different optical transitions between the bilayer graphene electronic bands and appears as a negative peak in the bandgap-opened bilayer graphene with respect to pristine bilayer graphene.[18] The electrical bandgap was also calculated from the on/off characteristics with following equation assuming the bandgap (E_g) of the bilayer graphene is double the size of the Schottky barrier height at charge neutral point (CNP).[19,36] $\Delta E_g = 2\Delta(\varphi_{barrier}) = 2(k_BT/q)\ln(I^0_{off}/I_{off})$, where ΔE_g is the increased bandgap, $\Delta\Phi_{barrier}$ is the difference in Schottky barrier heights, k_B is the Boltzmann constant, T is the temperature, I^0_{off} is the off current before molecular doping, and I_{off} is the off current after molecular doping. The calculated electrical bandgap with a thickness of F4-TCNQ layers increases from 65 to 124 meV with an increment rate of approximately 2.9 to 3.1 meV Å^{-1} (Figure 3d). Although the actual value of the electrical bandgap is lower than the optical bandgap, they share a similar trend. The discrepancy in the values of the optical and electrical bandgaps has been explained in previous reports, which agrees well with our measurement.[37] The electrical bandgaps tend to have smaller values due to the presence of the tunneling of carriers through defect sites.[19] However, the same increment rate of approximately 2.9 to 3.1 meV Å^{-1} in both the optical and electrical bandgaps supports our idea that the magnitude of the bandgap opening can be controlled by dual molecular doping.

When doping is only applied on top layer, the on/off current ratio also increases. To derive on/off current ratio, a drain current at $V_G = -100$ V is divided by that of minimum conductivity. However, the magnitude that uses single molecular doping is

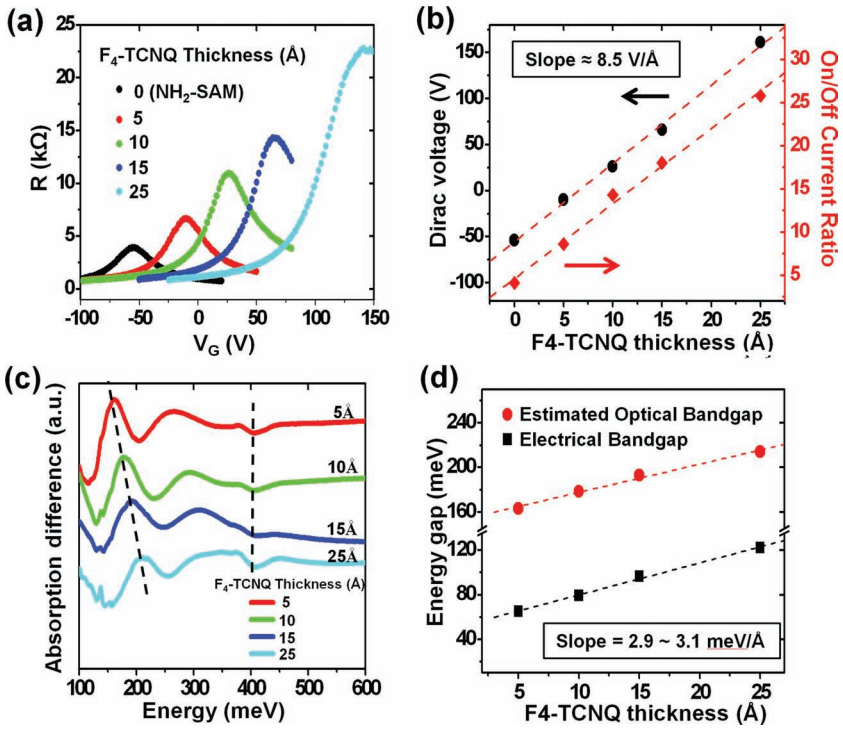

Figure 3. a) Current–voltage transfer characteristics of bilayer graphene FETs on a NH_2-SAM modified SiO_2/Si substrates with various thicknesses of the F4-TCNQ layers. b) Plots of the Dirac voltages and on/off current ratios with various thicknesses of F4-TCNQ layers. c) IR absorption spectra of bilayer graphene on NH_2-SAM modified SiO_2/Si substrates after deposition of various thickness of F4-TCNQ layers. The absorption spectrum of pristine bilayer graphene on bare SiO_2/Si substrate was subtracted as a background reference. d) The plots for electrical bandgaps and estimated optical bandgaps as a function of F4-TCNQ thickness.

much smaller than that of dual molecular doping (Supporting information Figure S2). Moreover, the position of the CNP (the location of maximum resistivity) of dual-doped bilayer graphene can be manipulated by controlling the degree of doping on each side independently, for example by varying the thickness of the F4-TCNQ. As shown in the output characteristics of bilayer graphene FETs with dual doping (Supporting Information Figure S3a–c), the device shows low off current after F4-TCNQ deposition. This result implies a consecutive opening of the bandgap with an increase in p-type doping from the top in combination with stable n-type doping at the bottom. Unlike the bandgap opening, the position of the CNP and resultant charge carrier density depends on the amount of effective doping, which can be derived from the compensation between the displacement fields exerted by the opposite types of dopants. The modulation of charge carrier density among different amount of effective doping is obvious when comparing the on currents of the output characteristics in Figure S3 (Supporting Information). This independent modulation of the position of the CNP is similar to dual-gated graphene transistors where the displacement field from the top and bottom gates breaks inversion symmetry while keeping the graphene charge neutral.[18] In the case of single molecular doping, on the contrary, doping of the graphene always increases the CNP, making it difficult to manipulate the CNP independently (Supporting Information Figure S2). This result implies that the dual doping method can provide a facile independent manipulation of the CNP and bandgap by introducing various combinations of opposite types of dopants at each side of graphene to control the degree of doping. Although the obtained on/off current ratio at room temperature (maximum value: ≈26) is not as high as the largest value reported (≈100),[19] the value is quite high compared to those based on single molecular dopants.[38] It should be noted that the use of dopants that do not incur disorder in the doping profile, for example, deposition of highly ordered molecules on a graphene surface,[39–42] can enhance the on/off current ratio much more while maintaining high field-effect mobility of graphene FETs.[38,43] Moreover, control of interface energetics with a metal electrode might decrease the on-state resistance so that the resulting on/off ratio can be enhanced.

To evaluate the stability of the devices, the Dirac voltages of bilayer graphene FETs on SAMs were monitored in a time-dependent manner. The Dirac voltage placed around –50 V did not shift after more than one month, confirming a stable n-doping effect with time. Since SAMs are chemically attached to the substrate and have strong van der Waals interactions among their hydrocarbon backbones, they are supposed to be stable under ambient conditions.[44] In the case of F4-TCNQ doping, strong p-doping indicates strong columbic interaction resulting from the formation of interface dipoles between F4-TCNQ molecules and graphene.[45] However, the stable doping is hampered by the degradation of F4-TCNQ molecules under ambient conditions by oxygen and water vapor. As a result, the Dirac voltage shifts slightly under ambient conditions. Interestingly, when we put the degraded samples in vacuum ($<10^{-6}$ Torr), the Dirac voltage and off resistance recovered to the original values. These results indicate that the proper passivation of the device can guarantee stable operation of bilayer graphene FETs.

In conclusion, we have investigated the effect of dual doping on the electrical properties of bilayer graphene FETs. Single-gate bilayer graphene FETs with high current on/off current ratios were successfully fabricated by dual molecular doping. In addition, the tunable bandgap was demonstrated by measuring optical transition of bilayer graphene with F4-TCNQ thickness and also supported by the calculation of the electrical bandgap. Our method shows that bandgap opening of bilayer graphene can be facilely accomplished by dual molecular doping, which does not require a complicated fabrication step for preparing the device with dual-gate structure.

Experimental Section

Materials and Device Fabrication: The NH_2-SAMs were constructed on SiO_2/Si substrate by immersing 3-aminopropyltrimethoxysilnae (10 mM) solution in toluene for 2 h. For the fabrication of bilayer graphene

transistors, mechanically exfoliated graphene flakes were prepared on a cleaned silicon substrate with a 300 nm SiO_2 layer (capacitance = 10.8 nF cm^{-2}) or a NH_2-SAM treated SiO_2/Si substrate. The source and drain electrodes (Au (50 nm)/Ti (5 nm)) were deposited with an e-beam evaporator after defining the patterns by e-beam lithography. Various thicknesses of F4-TCNQ layers were deposited on the graphene surface by thermal evaporator operating under high vacuum (10^{-6} Torr) with a uniform rate of 0.4 Å s^{-1}.

Characterization: The mechanically exfoliated bilayer graphene was identified by optical microscopy (Zeiss) and Raman spectroscopy (Renishaw, RM-1000 Invia) with an excitation energy of 2.41 eV (514 nm, Ar^+ ion laser). The optical bandgap was estimated by measuring the Fourier transform infrared (FT-IR) spectra of the F4-TCNQ/bilayer graphene/NH_2-SAM treated silicon substrate using a FT-IR spectrophotometer from Bruker Optik GMBH operating at the incident angle of 80°. To obtain large-area bilayer graphene for FT-IR characterization, chemical vapor deposition (CVD), which has been described in the literature, was used.[41,46] The portion of the CVD-grown bilayer graphene was well above 70% with a small portion of multilayer graphene, as characterized by optical microscopy. The Bernal stacking of the CVD-grown bilayer graphene was confirmed by Raman spectroscopy. The current–voltage characteristics were measured under vacuum conditions (10^{-3} Torr) using a Kiethley 2636A semiconductor parameter analyzer.

Supporting Information

Supporting Information is available from the Wiley Online Library or from the author.

Acknowledgements

This research was supported by the National Research Foundation of Korea (National honor scientist program, 2010-0020414; Future-based Technology Development Program, Nano Fields: 2010-0019128; Global Frontier Research Center for Advanced Soft Electronics; Converging Research Center Program 2010K001066, 2009-0089030l) funded by the Ministry of Education, Science and Technology.

Received: September 4, 2011
Revised: October 15, 2011
Published online: December 12, 2011

[1] K. S. Novoselov, A. K. Geim, S. V. Morozov, D. Jiang, M. I. Katsnelson, I. V. Grigorieva, S. V. Dubonos, A. A. Firsov, *Nature* **2005**, *438*, 197.
[2] Y. B. Zhang, Y. W. Tan, H. L. Stormer, P. Kim, *Nature* **2005**, *438*, 201.
[3] A. F. Young, P. Kim, *Nat. Phys.* **2009**, *5*, 222.
[4] C. R. Dean, A. F. Young, I. Meric, C. Lee, L. Wang, S. Sorgenfrei, K. Watanabe, T. Taniguchi, P. Kim, K. L. Shepard, J. Hone, *Nat. Nanotechnol.* **2010**, *5*, 722.
[5] Y. Q. Wu, Y. M. Lin, A. A. Bol, K. A. Jenkins, F. N. Xia, D. B. Farmer, Y. Zhu, P. Avouris, *Nature* **2011**, *472*, 74.
[6] L. Liao, Y. C. Lin, M. Q. Bao, R. Cheng, J. W. Bai, Y. A. Liu, Y. Q. Qu, K. L. Wang, Y. Huang, X. F. Duan, *Nature* **2010**, *467*, 305.
[7] K. S. Kim, Y. Zhao, H. Jang, S. Y. Lee, J. M. Kim, K. S. Kim, J. H. Ahn, P. Kim, J. Y. Choi, B. H. Hong, *Nature* **2009**, *457*, 706.
[8] W. H. Lee, J. Park, S. H. Sim, S. B. Jo, K. S. Kim, B. H. Hong, K. Cho, *Adv. Mater.* **2011**, *23*, 1752.
[9] S. Garaj, W. Hubbard, A. Reina, J. Kong, D. Branton, J. A. Golovchenko, *Nature* **2010**, *467*, 190.
[10] S. K. Min, W. Y. Kim, Y. Cho, K. S. Kim, *Nat. Nanotechnol.* **2011**, *6*, 162.
[11] M. Y. Han, B. Ozyilmaz, Y. B. Zhang, P. Kim, *Phys. Rev. Lett.* **2007**, *98*.
[12] X. L. Li, X. R. Wang, L. Zhang, S. W. Lee, H. J. Dai, *Science* **2008**, *319*, 1229.
[13] R. Balog, B. Jorgensen, L. Nilsson, M. Andersen, E. Rienks, M. Bianchi, M. Fanetti, E. Laegsgaard, A. Baraldi, S. Lizzit, Z. Sljivancanin, F. Besenbacher, B. Hammer, T. G. Pedersen, P. Hofmann, L. Hornekaer, *Nat. Mater.* **2010**, *9*, 315.
[14] P. A. Denis, *Chem. Phys. Lett.* **2010**, *492*, 251.
[15] E. McCann, *Phys. Rev. B* **2006**, *74*.
[16] E. V. Castro, K. S. Novoselov, S. V. Morozov, N. M. R. Peres, J. M. B. L. Dos Santos, J. Nilsson, F. Guinea, A. K. Geim, A. H. C. Neto, *Phys. Rev. Lett.* **2007**, *99*.
[17] J. B. Oostinga, H. B. Heersche, X. L. Liu, A. F. Morpurgo, L. M. K. Vandersypen, *Nat. Mater.* **2008**, *7*, 151.
[18] Y. B. Zhang, T. T. Tang, C. Girit, Z. Hao, M. C. Martin, A. Zettl, M. F. Crommie, Y. R. Shen, F. Wang, *Nature* **2009**, *459*, 820.
[19] F. N. Xia, D. B. Farmer, Y. M. Lin, P. Avouris, *Nano. Lett.* **2010**, *10*, 715.
[20] T. Taychatanapat, P. Jarillo-Herrero, *Phys. Rev. Lett.* **2010**, *105*.
[21] Y. Zhang, T. Mori, L. Niu, J. Ye, *Energy Environ. Sci.* **2011**, 4, 4517.
[22] T. Ohta, A. Bostwick, T. Seyller, K. Horn, E. Rotenberg, *Science* **2006**, *313*, 951.
[23] C. Coletti, C. Riedl, D. S. Lee, B. Krauss, L. Patthey, K. von Klitzing, J. H. Smet, U. Starke, *Phys. Rev. B* **2010**, *81*, 235401.
[24] R. Wang, S. N. Wang, D. D. Zhang, Z. J. Li, Y. Fang, X. H. Qiu, *ACS Nano* **2011**, *5*, 408.
[25] Z. Yan, Z. Z. Sun, W. Lu, J. Yao, Y. Zhu, J. M. Tour, *ACS Nano* **2011**, *5*, 1535.
[26] J. Park, W. H. Lee, S. Huh, S. H. Sim, S. B. Kim, K. Cho, B. H. Hong, K. S. Kim, *J. Phys. Chem. Lett.* **2011**, *2*, 841.
[27] A. C. Ferrari, J. C. Meyer, V. Scardaci, C. Casiraghi, M. Lazzeri, F. Mauri, S. Piscanec, D. Jiang, K. S. Novoselov, S. Roth, A. K. Geim, *Phys. Rev. Lett.* **2006**, *97*, 187401.
[28] K. H. Yim, G. L. Whiting, C. E. Murphy, J. J. M. Halls, J. H. Burroughes, R. H. Friend, J. S. Kim, *Adv. Mater.* **2008**, *20*, 3319.
[29] W. Chen, S. Chen, D. C. Qi, X. Y. Gao, A. T. S. Wee, *J. Am. Chem. Soc.* **2007**, *129*, 10418.
[30] X. Q. Tian, J. B. Xu, X. M. Wang, *J. Phys. Chem. B* **2010**, *114*, 11377.
[31] N. M. R. Peres, *Rev. Mod. Phys.* **2010**, *82*, 2673.
[32] F. Schedin, A. K. Geim, S. V. Morozov, E. W. Hill, P. Blake, M. I. Katsnelson, K. S. Novoselov, *Nat. Mater.* **2007**, *6*, 652.
[33] T. Lohmann, K. von Klitzing, J. H. Smet, *Nano. Lett.* **2009**, *9*, 1973.
[34] S. Adam, E. H. Hwang, V. M. Galitski, S. Das Sarma, *Proc. Natl. Acad. Sci. USA* **2007**, *104*, 18392.
[35] J. H. Chen, C. Jang, S. Adam, M. S. Fuhrer, E. D. Williams, M. Ishigami, *Nat. Phys.* **2008**, *4*, 377.
[36] W. Zhang, C.-T. Lin, K.-K. Liu, T. Tite, C.-Y. Su, C.-H. Chang, Y.-H. Lee, C.-W. Chu, K.-H. Wei, J.-L. Kuo, L.-J. Li, *ACS Nano* **2011**, *5*, 7517.
[37] H. Min, D. S. L. Abergel, E. H. Hwang, S. Das Sarma, *Phys. Rev. B* **2011**, *84*, 041406(R).
[38] B. N. Szafranek, D. Schall, M. Otto, D. Neumaier, H. Kurz, *Nano. Lett.* **2011**, *11*, 2640.
[39] Q. H. Wang, M. C. Hersam, *Nat. Chem.* **2009**, *1*, 206.
[40] T. Zhang, Z. G. Cheng, Y. B. Wang, Z. J. Li, C. X. Wang, Y. B. Li, Y. Fang, *Nano. Lett.* **2010**, *10*, 4738.
[41] G. Hlawacek, F. S. Khokhar, R. van Gastel, B. Poelsema, C. Teichert, *Nano. Lett.* **2011**, *11*, 333.
[42] E. Rossi, S. Das Sarma, *Phys. Rev. Lett.* **2011**, *107*, 155502.
[43] H. Miyazaki, K. Tsukagoshi, A. Kanda, M. Otani, S. Okada, *Nano. Lett.* **2010**, *10*, 3888.
[44] S. A. Di Benedetto, A. Facchetti, M. A. Ratner, T. J. Marks, *Adv. Mater.* **2009**, *21*, 1407.
[45] W. Chen, D. Qi, X. Gao, A. T. S. Wee, *Prog. Surf. Sci.* **2009**, *84*, 279.
[46] S. Lee, K. Lee, Z. Zhong, *Nano. Lett.* **2010**, *10*, 4702.